SPECIAL ISSUE ARTICLE

INNOVATION AND EMERGING TECHNOLOGIES

OPEN ACCESS

Placenta-on-a-chip: Response of neural cells to pharmaceutical agents transported across the placental barrier

Rajeendra L. Pemathilaka [1] & Nicole N. Hashemi [1,*]

Striving for sustainable drug discovery, we have presented a proof-of-concept for studying the effects of pharmaceutical agents transported across the placental barrier on neural cells. The potential effects of pharmaceutical agents on fetus have made concerns about their use and require more studies to address these concerns. A placenta-on-a-chip model was fabricated and tested for transport of naltrexone (NTX) and its primary metabolite 6β-naltrexol. The NTX/6β-naltrexol transported from the maternal channel to the fetal channel was then collected from the fetal channel. To evaluate the behavior of neural cells following exposure to NTX and 6β-naltrexol, perfusate from the fetal channel was directed toward the cultured N27 neural cells. Neural cells exposed to the transported NTX/6β-naltrexol were then evaluated for gene expression and cell viability. Results showed significantly higher fold changes in IL-6 and TNF-α expression when exposed to NTX/6β-naltrexol. However, a lower fold change in IL-1β expression was observed, while it remained the same in sphingosine kinase (sphk)1. Also, cell viability with NTX/6β-naltrexol exposure was determined to be significantly lower ($p < 0.001$). This study has the potential to reveal the impact of pharmaceutical agents on the developing neural system of fetuses and their premature brains.

***Keywords*: Placenta-on-a-Chip; Neural Cells; Placental Barrier.**

INTRODUCTION

It should come as no surprise that fetal drug exposure has been related to a wide range of neurological issues. Despite attempts at prevention and education, the current rate of illegal drug use among pregnant women aged 15–44 has remained stable at 5.9%[1]. Opioids are natural, synthetic, and semisynthetic mediators that can play an important role in the relief of chronic and severe pain. Neonatal abstinence syndrome (NAS), postnatal growth insufficiency, neonatal death, neurobehavioral disorders, and other related impairments have been reported in fetuses of women with opioid use disorder (OUD)[2]. Over 85% of pregnant women with OUD had unplanned pregnancies, with NAS affecting 3.39 out of 1,000 infants[1,3,4].

Naltrexone (NTX), which has very little addictive potential, is a widely accepted type of medicine used to treat opioid abuse. In order to have an effect, NTX opioid antagonist blocks μ-, κ-, and δ-opioid receptors, which reduces opioid craving and drug-seeking behavior[5,6]. Systolic dihydrodiol dehydrogenase breaks down NTX into 6β-naltrexol through the liver. 6β-Naltrexol is the main active metabolite of NTX, and it makes up to 43% of its pharmacological effects[5,7]. The effect of NTX and its metabolite 6β-naltrexol remains understudied and FDA is still undetermined about NTX effects during gestation and lactation[8,9]. In the previous study, the transfer of pharmaceutical agents like NTX and 6β-naltrexol through our placenta-on-a-chip model[10] was studied, and the effects of these agents on the behavior of endothelial and trophoblast cells were investigated in terms of gene expression[11].

To this date, we know of no placenta-on-a-chip study investigating the effect of NTX and 6β-naltrexol on the neural cells. Microfluidic devices[12–14] and organ-on-a-chip technologies[10,15] have been widely used in regenerative medicine and tissue engineering[16,17] as well as diagnostic studies[18–22]. In this study, a placenta-on-a-chip model with maternal and fetal channel was developed to mimic the placental barrier using human umbilical vein endothelial cells (HUVEC) and trophoblasts (BeWo) cells (**Fig. 1a–c**). Due to the fact that the BeWo cell line forms syncytium and be syncytialized upon treatment with cAMP or forskolin, it is utilized to examine placental function[23,24]. In vivo, the placental transport of maternal calcium (Ca^{2+}) is mediated by the syncytiotrophoblast layer. CaT1 and CaT2 expression is related with the Ca^{2+} uptake potential during the differentiation of cultured human trophoblasts obtained

[1]Department of Mechanical Engineering, Iowa State University, Ames, IA 50011, USA. *Correspondence should be addressed to: N.N.H. (nastaran@iastate.edu).

Received 4 December 2022; accepted 15 June 2023; published online 8 August 2023; doi:10.1142/S2737599423400042

This article is part of the "Special Issue on Organ-on-a-Chip Technologies", edited by Morteza Mahmoudi (Michigan State University, USA) & Vahid Serpooshan (Emory University School of Medicine and Georgia Institute of Technology, USA).

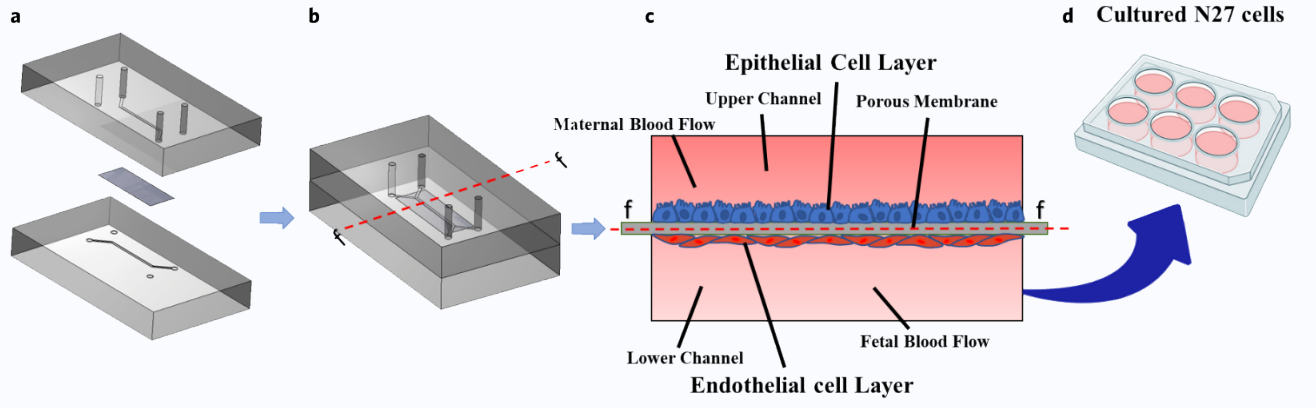

Figure 1 (**a**) Exploded view of the fabricated placenta-on-a-chip before microfluidic cell culture. The fabricated chip consists of two microchannel-etched PDMS layers, which is separated by a thin PETE membrane. (**b**) Assembled view of the fabricated placenta-on-a-chip model. (**c**) Cross-section of a placenta-on-a-chip device, with the endothelial cells in the fetal interface and the epithelial cells in the maternal interface, which are represented by HUVEC and BeWo cell layers. (**d**) Transferred perfusate from the maternal channel to the fetal channel being exposed to N27 cells.

from term placenta, according to studies. This association demonstrates the function of this family of channels in the syncytiotrophoblast's basal Ca^{2+} uptake. There is substantial evidence that fluid shear stress induces Ca^{2+} entrance into cells and causes the development of microvilli[11,25–28].

In the previous study, we demonstrated that fluid shear stress in our microfluidic device is an extracellular signal that induces syncytium development in BeWo cells without cAMP or forskolin administration[24]. We showed that in our microfluidic device, the shear stress was determined to be between 0.02 and 0.2 dyn/cm^2 in the microfluidic channel in which the cells were seeded. The BeWo cells in our developed placenta-on-a-chip model could have been syncytialized because to the continual exposure to fluid shear stress, since our prior research demonstrated a shear stress of 0.02–0.2 dyn/cm^2 on seeded cells[11].

NTX transfer through the placenta-on-a-chip model was previously studied[10,11]. The validity of these placenta-on-a-chip models is approved by previous studies[10,11]. Here, by transferring outflow from the fetal channel to cultured N27 embryonic-dopamine cells, we presented a proof-of-concept for sustainable modeling NTX and 6β-naltrexol transport to a fetus brain across the placental barrier (**Fig. 1a–d**). We also used a quantitative RT-PCR method to analyze gene expression changes that ensue from post-exposure to NTX and 6β-naltrexol. This work provides a platform for both the scientific and pharmaceutical communities to examine and extrapolate information regarding the safety and potential side effects caused by prescription opioid medication during pregnancy. More specifically, the knowledge gained should encourage other researchers to test and validate the short- and long-term effects NTX imposes on the mother's placental barrier and the fetus's premature brain.

METHODS

Design and fabrication of a placenta-on-a-chip device: The microchannels were fabricated in poly(dimethylsiloxane) (PDMS) using soft lithography techniques[19]. A mixture of PDMS prepolymer and curing agent (Sylgard 184; Dow Corning, MI) in the ratio of 10:1 (w/w) was poured on a SU-8 photoresist mold. A PETE membrane (0.4 µm pore size) was used as the barrier between the two microchannels (Corning®). Following the installation of inlet/outlet tubing to each channel, the chip was sterilized by UV for 20 minutes to ensure fluid access[11].

Cell culture in microfluidic systems: UV-sterilization was followed by coating the PETE membrane with Entactin-collagen IV laminin solution (10 g/mL in sterile serum-free media) through the channels. The next day, the microfluidic device's channels were flushed twice with phosphate-buffered saline (PBS), and the microchip was then ready for microfluidic cell culture. Trypsin/EDTA (1X) was used to dissociate both cell lines before infusion, and cells were again suspended in growth media, endothelial growth medium (EGM) and Ham's F-12K (Kaighn's) medium, prior to infusion. At a density of 5×10^6 cells/mL, the HUVECs were injected into the lower channel and incubated for 1 hour at 37°C with 5% CO_2 in the air to guarantee cell adhesion. A similar procedure was followed with a BeWo cell density of 5×10^6 cells/mL in the top channel, which was then connected to the lower channel through 3 mL Becton, Dickinson, and Company syringes loaded with EGM and F-12K media. The syringes were then connected to a syringe pump pumping EGM and F-12K media at a similar flow rate of 50 µL/h to the fetal and maternal channels, respectively[11].

CellTracker Orange and Green (Life Technologies) were used to stain BeWo and HUVEC cells, respectively. Both cell lines were cultured for 45 minutes with staining at 37°C with 5% CO_2 before being dissociated and stained in a diluted serum-free media. After establishing the growth of cells in the microchannels, immunohistochemistry was used to investigate the epithelial and endothelial integrity. After fixing the cultures in the maternal and fetal in 4% paraformaldehyde for 20 minutes, a blocking buffer (0.4% bovine serum albumin [BSA], 0.2% Triton X-100, and 5% normal donkey serum [Jackson ImmunoResearch Labs]) and normal donkey serum (5%) were incubated in the microchannels at room temperature for 60 minutes. Using anti-vascular endothelial cadherin (anti-VE-cadherin) and anti-epithelial cadherin (anti-E-cadherin) antibodies (#4412S and #8889S, Cell Signaling Technologies), the microchannels were treated at 4°C overnight with the primary antibodies for HUVECs and BeWo cells, respectively, before the blocking solution was added. PBS was washed from the microchannels the next day, followed by 90 minutes of incubation with secondary antibodies and DAPI solution, which were diluted with blocking serum. Finally, PBS was used to clean both microchannels, and the membrane was evaluated for immunostaining under a fluorescence microscope (Zeiss Axio Observer Z1)[11].

Stained BeWo cells were used to detect the growth of microvilli in the channels after 72 hours of proliferating cells within the channels. A PBS rinse was followed by 15 minutes of fixing the maternal channel with 4% paraformaldehyde, followed by a PBS rinse and 10 minutes of permeabilizing the channel cultures with 0.5% Triton X-100 at room

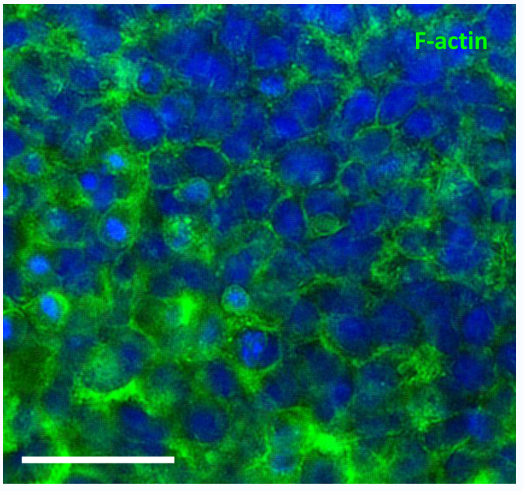

Figure 2 The formation of microvilli on the apical surface of the trophoblast was assessed by testing for the presence of filamentous actin (F-actin) protein. Scale bar: 50 μm.

temperature. CF® 488A-conjugated phalloidin (Biotium) (5 L of a 200 U/mL (in cell culture grade water) stock solution in 200 L of PBS) was used to stain the cultures after another PBS rinse. A Zeiss Axio Observer Z1 Microscope was used to image cells incubated for 20 after DAPI counterstaining[11]. A layer of microvilli was observed on the fluorescence microscopy images as shown in **Fig. 2**.

Since this study was carried out to demonstrate the potential of utilizing our placenta-on-a-chip system to learn about the transport of NTX and 6β-naltrexol across the placental barrier, we introduced an initial concentration of 100 ng/mL NTX and 6β-naltrexol (1:1) to the maternal channel. As a result, in the fetal channel, we achieved concentrations of about 2.5 ng/mL and 2.2 ng/mL for NTX and 6β-naltrexol, respectively.

The outflow from the fetal channel was directed toward N27 cells cultured in 6-well plates, and a live/dead assay was performed on the cells after 8 hours of continuous exposure to the following conditions: (a) Cells were maintained in RPMI 1640 medium with no exposure to outflow from the fetal channel. (b)

Cell culture: N27 embryonic-dopamine cell line was generously provided by Dr. Anumantha Kanthasamy at Iowa State University and was cultured in RPMI 1640 medium (Gibco), supplemented with 10% FBS, 2 mM L-glutamine (Gibco), and 100 U/mL penicillin and streptomycin (Gibco). Cell lines were incubated at 37°C with 5% CO_2 in air until they were 80%–90% confluent. After at least three passages, N27 cells were dissociated with trypsin/EDTA (1X) (Cascade Biologics) and plated into individual wells of a 6-well plate at a density of 25 × 10^3 cells/well[11].

Midbrain-derived embryonic N27 cell exposure to NTX and 6β-naltrexol: After 5 days of culture, the N27 cells in the 6-well plates were prepared for exposure to NTX and 6β-naltrexol. Following the NTX/6β-naltrexol-mixed F-12K perfusion, outflow of the fetal channel was directed to N27 cell-cultured individual wells of a 6-well plate. The treatment was performed for 8 hours after 1 hour of equilibrium phase, as described above. Three different experiment groups including two control conditions were used for data analysis under the following conditions: N27 cells cultured in RPMI 1640 medium and had no exposure to NTX and 6β-naltrexol, N27 cells (in RPMI 1640 medium) exposed to the outflow from the fetal channel without NTX and 6β-naltrexol in the system, and N27 cells (in RPMI 1640 medium) treated with NTX and 6β-naltrexol through the outflow of the microfluidic channel for 8 hours.

Quantitative RT-PCR: After exposure to NTX and 6β-naltrexol, N27 cells from 6-well plates were quantified using the RT-PCR method. After treatment, control and experimental samples were trypsinized, pelleted, and frozen at −80°C, then integrated into single-control and single-experimental sets before homogenization in TRIzol reagent (Invitrogen, Thermo Fisher) (trypsinized-HUVECs and -BeWo cells were perfused through channels and collected from outlets separately). Following homogenization, RNA isolation and reverse transcription were performed using the Absolutely RNA Miniprep kit (Stratagene) and cDNA synthesis system (Applied Biosystems), respectively. A Qiagen RT^2 SYBR Green master mix with validated qPCR human primers (for HUVECs and BeWo) or mouse primers (for N27 cells) from Qiagen (Frederick) was used to determine relative magnitudes of gene expression levels using RT-PCR. Human 18S rRNA or mouse 18S rRNA, the housekeeping genes, were used to normalize each sample, and melting curves and dissociation curves were constructed to verify the gathering of nonspecific amplicons-free peaks, as described in the manufacturer's recommended guidelines. The ΔC_t method developed to utilize threshold cycle (C_t) values from housekeeping gene and respective gene was used to calculate and report the results as a fold change in gene expression[29,30].

RESULTS

Characterization of the placenta-on-a-chip: A co-cultured microfluidic device was used in this study. As previously reported, HUVECs and BeWo were chosen to exhibit the cells at the fetal and maternal interfaces, respectively. To mimic the human placenta's endothelium and trophoblastic epithelium, HUVECs and BeWo cells were grown appropriately and seeded in their respective microfluidic channel. Once these cells demonstrated behavioral bonding and the formation of microvilli like placental structure, the maternal channel of the microfluidic device was exposed to NTX and 6β-naltrexol. The perfusate from the maternal channel to the fetal channel with mean fetal NTX and 6β-naltrexol concentrations of 2.50 ± 0.26 and 2.22 ± 0.25 ng/mL, was then collected[11].

N27 embryonic-dopamine cell line exposed to NTX and 6β-naltrexol: In this study, we proposed a possible concept for simulating effects on fetus brain cells from maternally administered NTX and 6β-naltrexol to the placenta-on-a-chip model. Since a previous study on pregnant mice reported that 6β-naltrexol enters the fetal brain at greater levels after promptly crossing the placental barrier, N27 cells were chosen as the neural cells[4].

A placenta-on-a-chip model was fabricated and co-cultured with endothelial and trophoblast cells. The maternal channel was exposed to NTX and its metabolite 6β-naltrexol. The transfer of these agents was previously investigated and the perfusate from the maternal channel to the fetal channel, which contained NTX/6β-naltrexol-mixed F-12K medium was collected then.

Initially, N27 cells, plated and cultured for 5 days, were exposed to NTX and 6β-naltrexol by simply directing the outflow of the fetal channel of the placenta-on-a-chip model, and two control condition measurements were also used to compare the results obtained from N27 cells exposed to NTX and 6β-naltrexol. Following an 8-hour transfer of perfusate to N27 cells cultured in 6-well plates, cells were stained with a live/dead cell assay. As indicated in **Fig. 3a, b**, fluorescent images displayed only minor cell death under both control conditions, while live/dead cell assays identified a large amount of cell death on the cell layer (**Fig. 3c**) exposed to the fetal channel from co-culture devices perfusing NTX and 6β-naltrexol.

To quantify cell viability, fluorescent images were analyzed by counting live and dead cells. Cell viability (**Fig. 4a**) exhibited no significant difference ($p > 0.05$) for both control studies, verifying minimal effects against cell apoptosis after N27 cells are exposed to EGM. In addition,

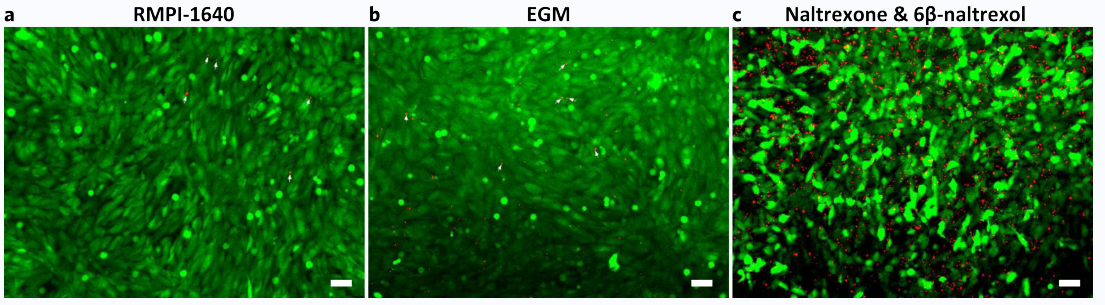

Figure 3 The outflow from the fetal channel was directed toward N27 cells cultured in 6-well plates, and a live/dead assay was performed on the cells after 8 hours of continuous exposure to the following conditions: (**a**) Cells were maintained in RPMI 1640 medium with no exposure to outflow from the fetal channel. (**b**) Cells (in RPMI 1640 medium) were exposed to the fetal-channel outflow from the co-culture devices that perfused NTX- and 6β-naltrexol-free medium through the maternal channel. (**c**) Cells (in RPMI 1640 medium) were exposed to NTX and 6β-naltrexol through the fetal-channel outflow from co-culture devices. Live and dead cells are indicated in green and red, respectively. Scale bars, 50 μm.

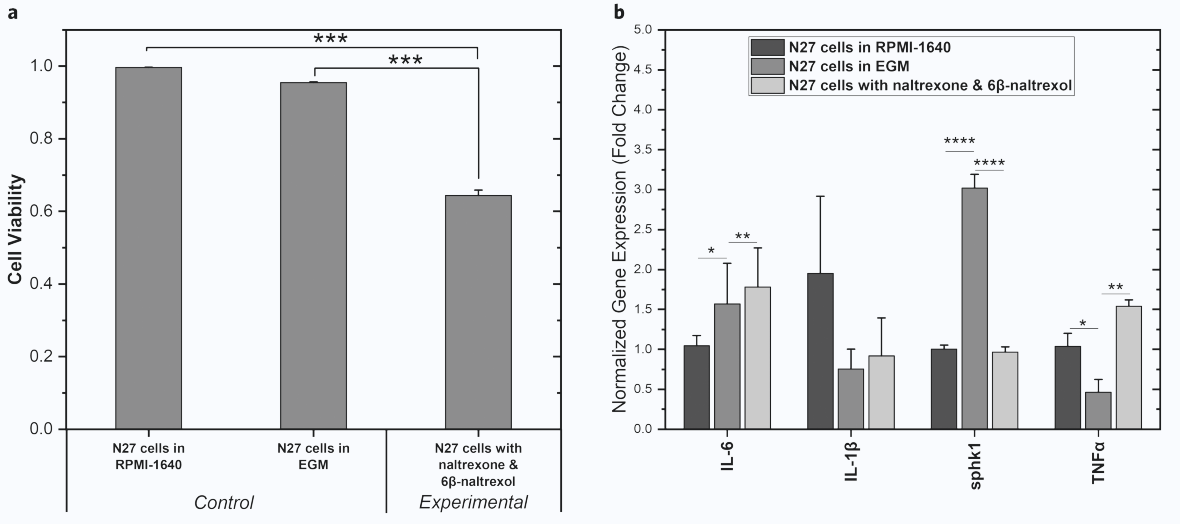

Figure 4 (**a**) Cell viability of N27 was examined in RPMI-1640, EGM, and with naltrexone and 6β-naltrexol. The data were calculated from 3 to 4 images. (**b**) Gene expression analysis on N27 cells subjected to conditions (RMPI-1640), (EGM), and (Naltrexone and 6β-naltrexol). The mouse 18S rRNA, the housekeeping gene, was referenced to report gene expression levels as a fold change. $n = 3$ independent experiments. Data are represented as the mean (± SEM). Scale bars, 50 μm. One-way ANOVA, $^{*}p < 0.05$; $^{**}p < 0.01$; $^{***}p < 0.001$; $^{****}p < 0.0001$.

an experimental study with N27 cells exposed to NTX and 6β-naltrexol showed a significant decrease in cell viability compared to cell viability found in both control studies ($p < 0.001$). We next evaluated N27 cells for genetic changes following post-exposure to NTX and 6β-naltrexol. As indicated in **Fig. 4b**, N27 cells were observed for IL-6, IL-1β, sphingosine kinase (sphk)1, and TNFα gene expressions.

DISCUSSION

It has been reported that IL-6 and IL-1β expression levels have produced increases in plasma levels of fetal brains[31], and acute inflammatory insult to a developing brain from IL-6 gene expression[32], and the possibility of TNF-α reducing embryonic development of the brain have also been reported[33]. sphk1 enzyme is associated with increasing survival and proliferation of cells[34], and sphk1 exhibits standard physiological functions in developing brain cells[35]. During this phase of the study, perfusate with the mean fetal concentrations of NTX and 6β-naltrexol over the 8-hour interval was recorded as 2.50 ± 0.26 and 2.22 ± 0.25 ng/mL, respectively[11], and was directed to investigate embryonic brain cells exposed to NTX and 6β-naltrexol. Following cell viability evaluation, cells were observed for IL-6, IL-1β, sphk1, and TNFα gene expressions. As it is shown in **Fig. 4b**, N27 cells exposed to NTX and 6β-naltrexol exhibited significantly higher

fold change levels in IL-6 compared to those under both control conditions, while the control conditions exhibited a significant difference ($p < 0.05$) in fold change levels for IL-6 gene expression. It has been reported that NTX significantly elevates the levels of IL-6 and IL-12 in mouse cells[36]. Fold change levels revealed lower expression levels of IL-1β in N27 cells exposed to EGM and NTX/6β-naltrexol compared to levels in N27 cells maintained in RPMI-1640, but no significant differences were observed. Interestingly, sphk1 gene expressed fold change levels measured in N27 cells in RPMI-1640 and N27 cells exposed to NTX and 6β-naltrexol remained virtually constant, while the levels for cells exposed to EGM showed a significantly higher fold change values compared to cells in RMPI-1640 and exposed to NTX and 6β-naltrexol (for both, $p < 0.0001$). This could be attributed to rapid cell growth in N27 cells when exposed to EGM, because extra growth factors in EGM could be promoting cell growth. Conversely, TNF-α gene exhibited significantly lower fold change values in N27 cells in RMPI-1640 were observed than in N27 cells exposed to NTX and its primary metabolite and EGM.

With enhanced detection through liquid chromatography/mass spectrometry (LC-MS), this proof-of-concept can be used to analyze the transport of ~2–10 ng/mL (clinically relevant plasma concentration for NTX) of NTX and 6β-naltrexol and its effects on a fetus and its premature brain. Further studies are warranted to validate these results achieved from gene expression analysis of N27 cells following post-exposure to NTX and 6β-naltrexol.

The placenta-on-a-chip microsystems have the potential to provide crucial insights into understanding how pharmaceutical agents such as NTX/6β-naltrexol impact the developing neural system and premature brains of fetuses.

ACKNOWLEDGMENTS

This work was partially supported by the National Science Foundation Grant 2014346. This research used the resources of the W. M. Keck Metabolomics Laboratory at Iowa State University. The authors would like to thank Dr. Wolfgang Sadee and Dr. John Oberdick at Ohio State University for the gift of naltrexone and 6β-naltrexol. We acknowledge the technical assistance by Dr. Anumantha Kanthasamy, Dr. Jie Luo, Dr. Alex Wrede, and Nima Alimoradi. We also thank Lasitha Kurukula Arachchi for illustrating the Table of Contents (ToC) entry.

DATA AVAILABILITY STATEMENT

The data that support the findings of this study are available from the corresponding author upon reasonable request.

DECLARATION OF COMPETING INTEREST

The authors declare no conflict of interest.

ORCID

Rajeendra L. Pemathilaka https://orcid.org/0000-0002-4347-8333
Nicole N. Hashemi https://orcid.org/0000-0001-8921-7588

REFERENCES

1. Saia, K.A. *et al*. Caring for pregnant women with opioid use disorder in the USA: Expanding and improving treatment. *Curr. Obstet. Gynecol. Rep*. **5**(3), 257–263 (2016).
2. Serra, A.E. *et al*. Delayed villous maturation in term placentas exposed to opioid maintenance therapy: A retrospective cohort study. *Am. J. Obstet. Gynecol*. **216**(4), 418.e1–418.e5 (2017).
3. Heil, S.H. *et al*. Unintended pregnancy in opioid-abusing women. *J. Subst. Abuse Treat*. **40**(2), 199–202 (2011).
4. Oberdick, J. *et al*. Preferential delivery of an opioid antagonist to the fetal brain in pregnant mice. *J. Pharmacol. Exp. Ther*. **358**(1), 22–30 (2016).
5. Morello, C.M. *et al*. Naltrexone metabolism and concomitant drug concentrations in chronic pain patients. *J. Anal. Toxicol* **38**(4), 212–217 (2014).
6. Tompkins, C.N.E. *et al*. Factors influencing recruitment to a randomised placebo-controlled trial of oral naltrexone and extended release implant naltrexone: Qualitative study. *J. Subst. Abuse Treat*. **99**, 52–60 (2019).
7. Bilsky, E. *et al*. 6β-naltrexol, a peripherally selective opioid antagonist that inhibits morphine-induced slowing of gastrointestinal transit: An exploratory study. *Pain Med*. **12**(12), 1727–1737 (2011).
8. Tran, T.H. *et al*. Methadone, buprenorphine, and naltrexone for the treatment of opioid use disorder in pregnant women. *Pharmacotherapy: J. Hum. Pharmacol. Drug Ther*. **37**(7), 824–839 (2017).
9. Rodriguez, C.E. & Klie, K.A. Pharmacological treatment of opioid use disorder in pregnancy. *Semin. Perinatol*. **43**(3), 7 (2019).
10. Pemathilaka, R.L. *et al*. Placenta-on-a-chip: In vitro study of caffeine transport across placental barrier using liquid chromatography mass spectrometry. *Global Chall*. **3**(3), 1800112 (2019).
11. Pemathilaka, R.L., N.A., Reynolds, D.E. & Hashemi, N.N. Transport of maternally administered pharmaceutical agents across the placental barrier in vitro. *ACS Appl. Bio Mater*. **5**, 2273–2284 (2022).
12. Hashemi, N. *et al*. A paper-based microbial fuel cell operating under continuous flow condition. *Technology* **4**(2), 98–103 (2016).
13. Sechi, D. *et al*. Three-dimensional paper-based microfluidic device for assays of protein and glucose in urine. *Anal. Chem*. **85**(22), 10733–10737 (2013).
14. Niaraki, A. *et al*. Graphene microelectrodes for real-time impedance spectroscopy of neural cells. *ACS Appl. Bio Mater*. **5**, 113–122 (2022).
15. Caplin, J.D. *et al*. Microfluidic organ-on-a-chip technology for advancement of drug development and toxicology. *Adv. Healthc. Mater*. **4**(10), 1426–1450 (2015).
16. Sharifi, F. *et al*. Polycaprolactone microfibrous scaffolds to navigate neural stem cells. *Biomacromolecules* **17**(10), 3287–3297 (2016).
17. Sharifi, F. *et al*. Photo-cross-linked poly (ethylene glycol) diacrylate hydrogels: Spherical microparticles to bow tie-shaped microfibers. *ACS Appl. Mater. Interfaces* **11**(20), 18797–18807 (2019).
18. Aykar, S.S. *et al*. Microfluidic seeding of cells on the inner surface of alginate hollow microfibers. *Adv. Healthc. Mater*. **11**, 2102701 (2022).
19. Bai, Z. *et al*. On-chip development of hydrogel microfibers from round to square/ribbon shape. *J. Mater. Chem. A* **2**(14), 4878–4884 (2014).
20. McNamara, M.C. *et al*. Behavior of neural cells post manufacturing and after prolonged encapsulation within conductive graphene-laden alginate microfibers. *Adv. Biol*. **5**(11), 2101026 (2021).
21. McNamara, M.C. *et al*. Targeted microfluidic manufacturing to mimic biological microenvironments: Cell-encapsulated hollow fibers. *ACS Macro Lett*. **10**(6), 732–736 (2021).
22. McNamara, M.C. *et al*. Microfluidic manufacturing of alginate fibers with encapsulated astrocyte cells. *ACS Appl. Bio Mater*. **2**(4), 1603–1613 (2019).
23. Msheik, H. *et al*. Transcriptomic profiling of trophoblast fusion using BeWo and JEG-3 cell lines. *Mol. Hum. Reprod*. **25**(12), 811–824 (2019).
24. Lecarpentier, E. *et al*. Fluid shear stress promotes placental growth factor upregulation in human syncytiotrophoblast through the cAMP–PKA signaling pathway. *Hypertension* **68**(6), 1438–1446 (2016).
25. Moreau, R. *et al*. Expression of calcium channels along the differentiation of cultured trophoblast cells from human term placenta. *Biol. Reprod*. **67**(5), 1473–1479 (2002).
26. Ando, J. & Yamamoto, K. Flow detection and calcium signalling in vascular endothelial cells. *Cardiovasc. Res*. **99**(2), 260–268 (2013).
27. Miura, S. *et al*. Fluid shear triggers microvilli formation via mechanosensitive activation of TRPV6. *Nat. Commun*. **6**(1), 1–11 (2015).
28. Abostait, A. *et al*. Placental nanoparticle uptake-on-a-chip: The impact of trophoblast syncytialization and shear stress. *Mol. Pharmaceutics*. **19**, 3757–3769 (2022).
29. Livak, K.J. & Schmittgen, T.D. Analysis of relative gene expression data using real-time quantitative PCR and the 2-ΔΔCT method. *Methods* **25**(4), 402–408 (2001).
30. Neal, M. *et al*. Prokineticin-2 promotes chemotaxis and alternative A2 reactivity of astrocytes. *Glia* **66**(10), 2137–2157 (2018).
31. Nadeau-Vallée, M. *et al*. Antenatal suppression of IL-1 protects against inflammation-induced fetal injury and improves neonatal and developmental outcomes in mice. *J. Immunol*. **198**(5), 2047–2062 (2017).
32. Wu, W.-L. *et al*. The placental interleukin-6 signaling controls fetal brain development and behavior. *Brain Behav. Immun*. **62**, 11–23 (2017).
33. Chao, C.C. & Hu, S. Tumor necrosis factor-alpha potentiates glutamate neurotoxicity in human fetal brain cell cultures. *Dev. Neurosci*. **16**(3–4), 172–179 (1994).
34. Olivera, A. *et al*. Sphingosine kinase expression increases intracellular sphingosine-1-phosphate and promotes cell growth and survival. *J. Cell Biol*. **147**(3), 545–558 (1999).
35. Lin, H. *et al*. Expression of sphingosine kinase 1 in amoeboid microglial cells in the corpus callosum of postnatal rats. *J. Neuroinflammation* **8**(1), 13 (2011).
36. Matters, G.L. *et al*. The opioid antagonist naltrexone improves murine inflammatory bowel disease. *J. Immunotoxicol*. **5**(2), 179–187 (2008).